A Simple Electric Soft Robotic Gripper with High-Deformation Haptic Feedback

Lillian Chin[1], Michelle C. Yuen[2,3], Jeffrey Lipton[1,4], Luis H. Trueba[1], Rebecca Kramer-Bottiglio[2], and Daniela Rus[1]

***Abstract*— Compliant robotic grippers are more robust to uncertainties in grasping and manipulation tasks, especially when paired with tactile and proprioceptive feedback. Although considerable progress has been made towards achieving proprioceptive soft robotic grippers, current efforts require complex driving hardware or fabrication techniques. In this paper, we present a simple scalable soft robotic gripper integrated with high-deformation strain and pressure sensors. The gripper is composed of structurally-compliant handed shearing auxetic structures actuated by electric motors. Coupling deformable sensors with the compliant grippers enables gripper proprioception and object classification. With this sensorized system, we are able to identify objects' size to within 33% of actual radius and sort objects as hard / soft with 78% accuracy.**

I. INTRODUCTION

Robot grasping and manipulation are critical to future interaction with humans in real world situations, such as home assistance or elderly care. However, everyday tasks can be quite difficult for traditional rigid manipulators because of the unstructured environments and diversity of objects encountered in everyday operation. The intrinsic compliance of soft robots allows them to tolerate these uncertainties. Their lower stiffness and continuous deformation allow soft manipulators to more deftly grasp a wider range of objects without complex control schemes or obstacle avoidance measures [1, 2]. Soft grippers can further exploit their environmental interaction with the addition of soft haptic sensing, allowing greater understanding of the grasped object and external deformations of the hand itself [3].

Considerable progress has been made in creating these proprioceptive soft robotic grippers [4]. Current approaches include adding off-the-shelf components to the rigid components of a compliant gripper [5], embedding sensors within the soft body of the hand [6, 7], or directly building sensors through the manufacturing process [8, 9]. However, these solutions do not fully deliver on the potential of soft grippers due to their bulky actuation schemes and fabrication methods. Most of these grippers rely on pneumatic actuation due to its fast response time and high strength-weight ratio. However, the need for a pump, compressor and valves to convert electric power to fluidic systems adds considerable physical bulk and power inefficiencies [10]. This issue of complex driving hardware is present in other popular actuation schemes like cable-driven and shape memory alloy systems [11]. The single-material solutions avoid this overhead of complex assembly, but rely on bespoke manufacturing processes with low throughput, making their potential adoption limited [12]. There is a clear need for a soft robotic gripper designed with scalable actuation and fabrication methods.

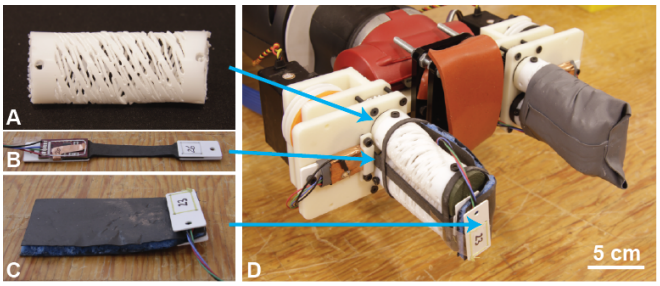

Fig. 1. Overview of the overall gripper design. Each finger of the gripper is actuated by a servo to a pair of handed shearing auxetic cylinders (A). An elastic strain sensor along the outer curve of the finger provides proprioceptive feedback (B). A pressure sensor along the inner curve provides haptic sensing (C). We demonstrate how these components fit together on the gripper by removing the glove from the left finger (D).

To address this need, we present a fully electric, sensorized soft robotic gripper fabricated via scalable manufacturing techniques. By combining the compliance of the handed shearing auxetic (HSA) structures from [13] and the highly-deformable strain and pressure sensors from [14], our gripper is able to measure its own large deformation proprioceptively. This allows it it to sense the difference between stiff vs. soft objects and large vs. small objects, similar to how humans understand an object's stiffness through the combination of the feel of an object and the inherent knowledge of the softness of our own fingertips and hands. We characterize this proprioception, detecting a finger bending angle of up to 45° and identifying grasped objects' diameter and stiffnesses. The main contributions of this paper are:

- creation and characterization of an electrically-driven soft HSA-based robotic gripper with integrated soft strain and pressure sensors
- a simple regression-based model that can estimate the radius of grasped objects to within 33% and distinguish hard vs. soft objects with 78% accuracy

[1] Computer Science and Artificial Intelligence Lab, Massachusetts Institute of Technology, Cambridge, MA, USA. email: {ltchin, jlipton, trueluis, rus}@csail.mit.edu

[2] School of Engineering and Applied Science, Yale University, New Haven, CT, USA. email: {michelle.yuen, rebecca.kramer}@yale.edu

[3] School of Mechanical Engineering, Purdue University, West Lafayette, IN, USA.

[4] Mechanical Engineering Department, University of Washington, Seattle, WA, USA.

II. RELATED WORK

Proprioceptive soft robotic manipulators generally fall under one of two categories: (1) compliant grippers built from rigid materials and flexible drivetrains [15–17] and (2) fluid-driven grippers made directly out of soft materials, typically, silicone elastomers [1].

The majority of efforts to incorporate sensing into rigid-material, compliant grippers have leveraged pressure-sensitive pads on the fingertips for force feedback [5, 18] or for classifying the grasped object based on size and orientation [19, 20]. Joint angle sensors have also been used to reconstruct the pose of the gripper [5, 21]. While the capabilities of these grippers have been enhanced by the incorporation of haptic feedback, they remain limited by the existence of rigid linkages and pre-defined joints.

Soft material-based grippers, however, leverage the softness of the actuation scheme and their bulk material properties to create a fully compliant system [1]. These grippers tend to be fluid-driven with interior chambers that upon addition / removal of fluid, close up and grasp around an object. Efforts towards sensorizing soft material grippers have utilized liquid metal-based deformation sensors to track motion of the gripper fingers [9, 22, 23], conductive elastomer-based strain and pressure sensors for haptic-based mapping of object contours [24], commercially-available bend sensors to classify objects [6], and either conductive elastomer or liquid metal-based sensors to control the degree of grasp of the gripper [14, 25]. While these soft material grippers have demonstrated success in passively conforming to grasp objects, a fluid-driven actuation system can be unwieldy and difficult to implement. Hence, despite competent sensory feedback, the complexity of the actuation scheme limits the utility of the sensor information and the ultimate applicability of soft-material grippers in real-world environments.

In this work, we integrate a rigid-material, yet compliant gripper structure with soft-material strain and pressure sensors. By using the HSAs, our gripper is motor-driven like rigid articulated systems, allowing us to avoid the issues of controlling infinite degrees of freedom commonly found in purely soft systems. The stretchability of the sensors allows the large deformations (50% strain) of the HSAs to be measured. The design of both the HSAs and the sensors are highly dependent on their constituent materials, much like how conventional fluidic soft robots leverage the extreme stretchability of their materials to create motion. The coupled choices of material and design allow us to create a compliant, sensorized gripper with a simple design and actuation scheme, and efficient use of materials.

III. GRIPPER DESIGN

To address gaps in current research, our primary design requirements (DRs) for this gripper were:

1) a compliant system
2) directly electrically powered
3) scalable fabrication techniques
4) proprioceptive / tactile sensing

Our final gripper design (Fig. 1) achieved these goals by combining the compliant electric actuators shown in [13] with the stretchable strain and pressure sensors demonstrated in [14] to create a versatile novel gripper. The gripper is made up of two fingers that pinch together, with each finger comprising a pair of HSA cylinders of opposite chiralities that counterrotate against each other, driven by a multi-turn servo. The strain and pressure sensors were then mounted on to each finger via 3D-printed caps and adapters. The pressure sensors were placed along the inner curve of the fingers, while the strain sensors were placed on the outer curve. Since the sensors deform with the fingers, the effect on overall displacement is minimal.

Each finger was then mounted to a 3D-printed adapter made to fit a Rethink Robotics Baxter robot used for manipulation. The distance between the fingers was determined by the mounting points of the Baxter, giving a open finger distance of 9.5 mm. To add a third point of contact, a 5 mm wide silicone-covered palm was mounted between the two fingers. Per DR3, this gripper is only made via standard manufacturing techniques, such as laser cutting, rod-coating, fused deposition modeling 3D printing, and silicone casting.

A. Actuator Selection

In order to have actuators that satisfy design requirements 1-3, we chose the compliant electric actuators demonstrated in [13] that are based on handed shearing auxetics. HSAs expand on traditional auxetics (materials with a negative Poisson's ratio) by having a set chirality and net shear. Thus, HSAs directly couple twisting motion with linear extension. When two HSA cylinders of opposite chirality are paired together, each cylinder opposes the other's direction of twisting, allowing the pair to extend as a unit [26].

HSAs were the ideal actuators for our system because by using traditional motors and servos, linear actuation and bending can be achieved, directly satisfying DR2. Furthermore, since any material that can support a pin joint or living hinge joint can exhibit HSA material properties, we had significant design space and possible material selection to achieve our desired level of compliance, addressing DR1.

For the cylinders in our gripper, we laser cut 60 mm long, 25.6 mm diameter PTFE tubes with a 1.58 mm wall thickness on a rotary engraver (PLS6.150D, Universal Laser Systems). We cut our tubes with a tessellated pattern similar to [27] with six base units around the circumference. To grasp objects, we added an internal constraint layer to the pattern to allow out-of-plane bending similar to the standard pneunet actuator [28].

B. Sensor Selection

Once we were set on using an HSA-based gripper design, the best sensor for our design goals were the strain and pressure sensors originally presented in [29] and [14]. Each sensor is based on a capacitive stack-up of a conductive charging layer, dielectric layers and conductive shielding ground layers [30]. When stretched, the overlapping area between the charging and ground layers increases, while the

dielectric layer becomes thinner, resulting in an increase in capacitance. A similar effect occurs in the pressure sensors as they are compressed.

These sensors were ideal for our gripper as they could match the high deformations of the HSAs and provide reliable results. By being soft themselves, the sensors would increase finger conformation around a grasped object without inhibiting any finger movement. The strain sensors had also previously been shown to have a linear response to their intended mechanical parameter over thousands of cycles, ensuring that they would still reliably work for the lifetime of the gripper [29].

The strain sensors in this paper were made from a five-layer capacitive stack-up while the pressure sensors were a three-layer stack-up (no ground shielding). The conductive layers were made of an expanded graphite and silicone composite material. The dielectric layers were silicone elastomer (DragonSkin 10 Slow, Smooth-On) for the strain sensors, and a porous ($\approx$ 65%) foam made from silicone and sacrificial sugar pellets (Suglets, Colorcon). Each sensor was interrogated using a signal conditioning board which charges the capacitor for a fixed amount of time, and then measures the length of time it takes to discharge to 0.2 V. This discharge time is a proxy for the capacitance, which in turn is a measure of the deformation applied.

Since there was significant electromagnetic interference from the servos, extra shielding was applied to the sensors in the form of a thin (1/32") silicone glove and copper tape. This glove also helped hold the sensors in place and increase contact friction between the gripper and grasped object. An extra infinite impulse response filter was also applied to the sensor reading to reduce noise outputs at the cost of a more delayed response time.

IV. GRIPPER CHARACTERIZATION

When the gripper grasps an object, the grasped object places external forces on the soft gripper, causing extra deformation. We characterized the gripper in a non-grasping environment in order to recognize these extra deformations and use them for object size sorting (Fig. 2).

To connect our knowledge of given servo position, strain sensor reading and overall finger bend radius, we track the top and bottom caps of the unsheathed finger in an Optitrack motion capture system while stepping each of the servos from maximum open to maximum close back to maximum open. The maximum open state of the finger was when the internal living hinges were fully jammed against one another. The maximum closed state of the finger was when the finger began undergoing helical instability and twisted in on itself. This instability is due to manufacturing variance between the two cylinders, as one cylinder may be slightly more compliant than another due to variations of the internal beam widths and living hinge thicknesses.

Our reference frame in the Optitrack system is defined by the coordinate system defined by the bottom cap, with X pointing into the page, Y pointing vertically, and Z pointing to the right of the figure. We measure the total movement

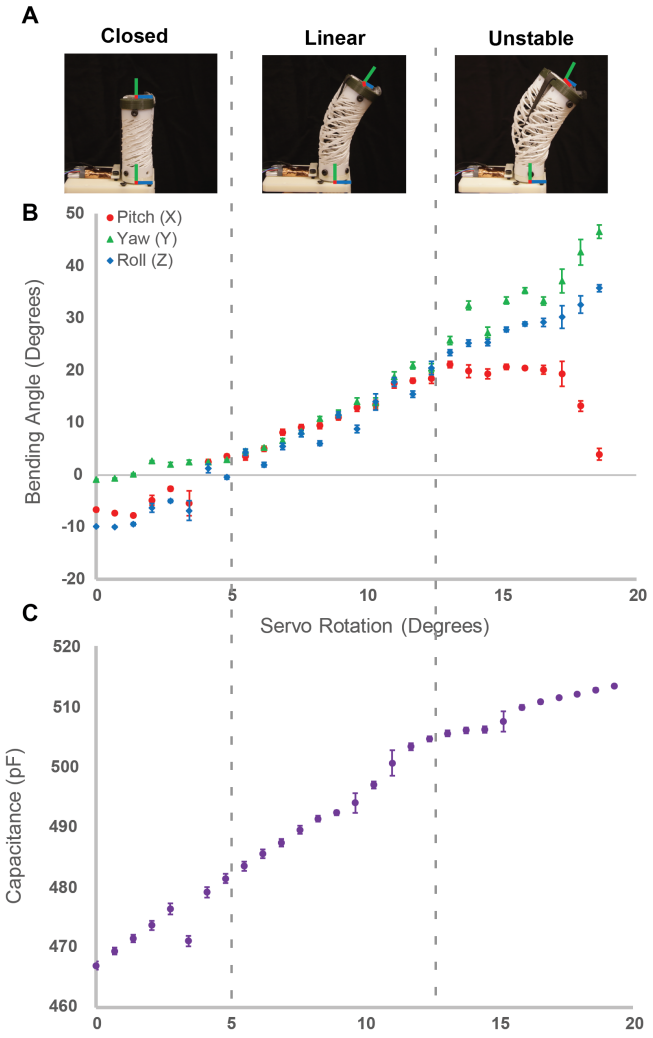

Fig. 2. Characterization of a single finger without load, which match the three states of the handed shearing auxetics – closed, linear regime and helical instability (A). We correspond the servo position to the overall bending angle (B) and the on-hand strain sensor (C). The bending angle is measured by taking the difference between the bottom and top plate's reference frames, as visualized in (A).

of the system by tracking how the reference frame of the moving top cap of the finger moves in relation to the coordinate system of the bottom cap. Initially, both reference frames coincide, but as the finger moves, the top reference frames rotates about the bottom reference frame. The top reference frame always has Y perpendicular to the plane created by the top of the top cap, which is spanned by the X and Z axes.

We conducted three open-close-open trials, giving us two datapoints per trial for a given servo angle. For a given servo rotation, we report the mean and standard deviation of all six data points. Although we only report results for the left finger here due to space, similar results can be found for the right finger. The only changes are that the servo turns in the opposite direction due to differences in chirality, and

that the strain sensors report a slightly different value at rest. The overall structure remains the same.

From these trials, we found a fairly linear correlation between the servo, the strain sensor and the overall geometry of the system (Fig. 2) (R^2 values vary from 0.931 to 0.974). As the servo rotates from its closed state to 13 degrees, the fingers elongate linearly up to about 25 degrees of bending radius. This linear elongation is expected as the finger constraint forces a constant curvature response from the fingers. At the 25 degree mark, we see the beginnings of the helical instability of the HSAs come in, resulting in a twisting of the actuators in on itself, stopping bending at nearly 45 degrees and leading to a pitch of 20 degrees (Fig. 2A). The strain sensor is able to capture this bending and twisting quite well, matching the linear growth in angle, tapering off after 15 degrees of servo rotation (Fig. 2B).

Since the rest state of the fingers (where top and bottom caps align) is at roughly 3 degrees of servo rotation, we see several anomalous values. The negative bending angle values from 0 - 3 degrees of servo rotation is an artifact of measuring the overall rotation angle as the difference between the top and bottom cap. Similarly, the anomalous sensor reading at 3 degrees bending angle is an artifact of the time averaging across datapoints. Thus, the strain sensors offer a good model of the state of the HSAs and can be used to approximate the state of the gripper.

V. OBJECT SORTING

To get a better sense of the sensor values in actual grasping use, we grasped a series of test objects with known stiffnesses and geometries and recorded the sensor readings during grasping (Fig. 3). We are interested in evaluating how well the gripper can bucket different objects into categories of "large vs. small" and "soft vs. stiff", similar to human categorization.

Our manipulation targets (Fig. 4) were drawn from the YCB Dataset [31] and other sources to get a wide range of compliance (1 - 10^3 MPa) and size (20 - 55 mm in radius). For each object, we measured the cross sectional diameter and had three people rate the compliance of each object on a 1-10 scale, 10 being the most compliant. The average of these measurements was taken as the overall compliance of the object.

We chose to evaluate compliance on a simplified human-rated scale rather than Young's modulus or weight to more closely simulate human proprioception of classifying objects by binning on a scale. Furthermore, since the pressure sensors directly measure the grasp normal force, stiffness and weight only provide a partial capture of the actual overall compliance of the object. Objects with the same human compliance rating may not be the same stiffness, but fall into the same "hard" or "soft" categorization.

To minimize variance involved in grasp planning, we placed all of our objects manually in a set grasping configuration and had Baxter run through a preset grasping routine. Preset servo values are used for the gripper's open and closed states. After the gripper closed, the pressure and strain values are recorded. Each object is then picked up and shaken to determine robustness of grasp hold. We recorded data before shaking as the extra motion caused shifts in the grasping normal forces, changing the pressure sensor values dramatically. Although this pressure differential between the two fingers could be used for future object pose estimation, this is outside the current scope of the paper.

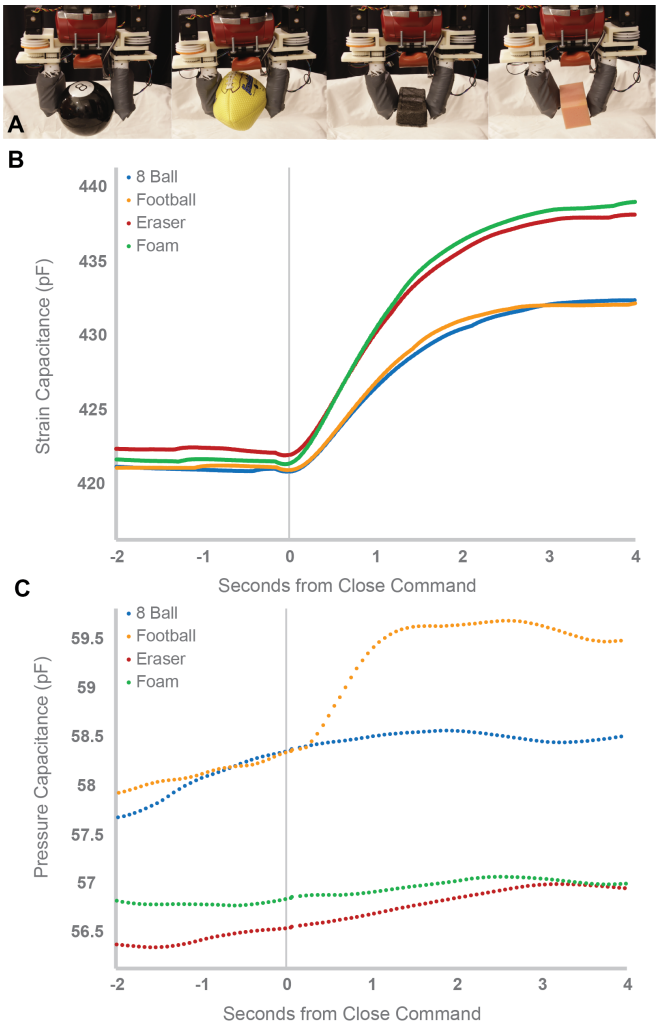

Fig. 3. Four representative objects grasped (A) and the corresponding strain (B) and pressure data (C) received from the sensors on the right finger. These objects were chosen as they represent the extremes of our datasets' compliance and size.

To get a baseline from which to evaluate the rest of the objects in terms of our four parameters (small, large, stiff and soft), we select four representative items – a magic 8 ball (compliance 1.3, diameter 107 mm), a deflated football (compliance 8.7, diameter 89 mm), a foam brick (compliance 9, diameter 43 mm) and a whiteboard eraser (compliance 2.3, diameter 51 mm) – and measured the sensor response (Fig. 3).

From the strain sensor, we see that the smaller objects had similar strain profiles as the fingers are able to mostly achieve their normal closed state. The slowly rising sensor response

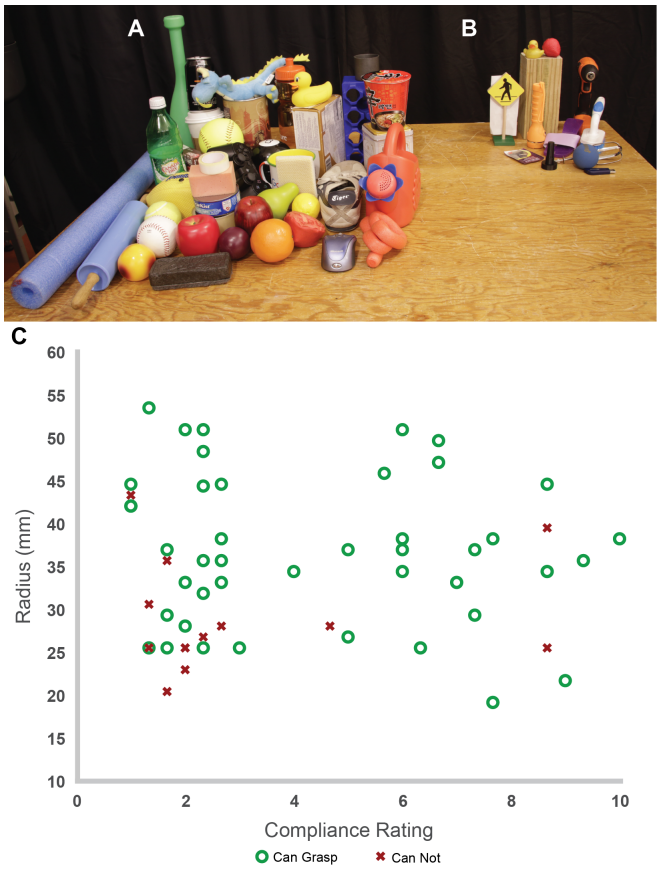

Fig. 4. Objects used in grasp testing. Our gripper could pick up the 43 objects in group (A) and could not pick up the 13 objects in group (B). Plotting compliance rating vs. radius reveals that our gripper has most difficulty with small stiff items (C), due to the larger force necessary to hold a small graspable area stably

stems from the sensor's transition to a higher strain as well as the increased noise filtration. The two larger objects caused a lower strain in the sensors as the fingers remained mostly open from the large object. We do note, however, that the strain sensors can not meaningfully tell the difference in cross section between the two large objects (a difference of 18 mm), while there is a small difference in strain between the smaller objects (a difference of 8 mm).

From the pressure sensor, we found that the larger objects have a much higher response than the smaller objects. This is probably due to the increased contact these objects have with the pressure sensor, causing the dielectric to compress over a larger area and the capacitance to increase. For a similar reason, it seems that for a given object size, more compliant objects tend to have a higher measured pressure as they can conform more easily to the pressure sensor, leading to an increase in affected area. We see this dramatically by comparing the football's reading to the 8-ball. However, as the item gets smaller, the contact footprint with the gripper shrinks as well. Since smaller objects tend to be grasped with a pinch grasp rather than a power grasp, the resulting effect on capacitance also tends to be diminished. Thus, we can estimate compliance for large objects more effectively than for smaller ones.

Using the results from the representative objects, we linearly interpolated the strain sensor values for the representative objects to allow our program to estimate size. We then used this size estimate with the pressure sensor readings to provide an estimate of compliance, performing a linear interpolation with a factor for size. We then ran grasping tests on the other 52 objects in our data set and recorded estimated size and stiffness.

In our experiments, we were able to grasp 77% of the 56 objects tested (Fig. 4). We generally had difficulty with small stiff objects which required pinch grasps (ex. plastic strawberry, small rubber duck) and heavy objects (ex. wood, drill). While small objects in general were difficult for our gripper due to the smaller area of graspable regions, small stiff objects were even more difficult as they needed a larger force to hold stably. Similarly, the weight of the heavier objects would be larger than the contact friction, causing the object to slip out of grasp. We could improve our grasping with both sets of objects by reducing slip – whether by closing the gripper more completely, increasing the gripper's contact friction, increasing the grasping force, or sensing slip directly.

Of the objects we could grasp, since the estimates were built off of an interpolation of four object sensor readings, we noted a wide range of estimated compliance that affected our evaluation. For very soft objects, our estimated compliance coefficient often was greater than 10, so we capped those values at 10. We also found that objects with metal in them reported an extremely large negative estimated compliance rating, ranging from -18 to -91. Since our sensors are based around capacitive sensing, coming into contact with metal objects would overwhelm our sensors and provide a nonsensical response. This effect was present even in objects with a slight amount of metal that was covered by plastic (ex. video game controller, coffee tin). While this effect could be useful for future object sorting, especially since living tissue also modifies the capacitance significantly, objects with negative compliance ratings (7 in total) were not used in our evaluation of the estimated compliance rating. These objects were still used in radius evaluation since the strain sensors did not come into contact with objects.

From the 43 objects we could grasp, we were able to estimate the cross sectional radius to within 33% accuracy (Fig. 5A). Our system had a slight bias, tending to underestimate the radius of objects with radius lower than 30 mm, and overestimating the radius of objects with radius greater than 40 mm. This effect may be an artifact from the linear interpolation performed from the four representative objects and may be mitigated with a more complex interpolation.

From the 36 non-metal objects we could grasp, we were able to tell the difference between hard and soft objects with 78% accuracy (p-value $= 0.0003$) (Fig. 5B), where soft objects were defined as those with compliance rating below 5 (the midpoint of our rating system). A binary classification was used to evaluate our classifier as the capped estimated

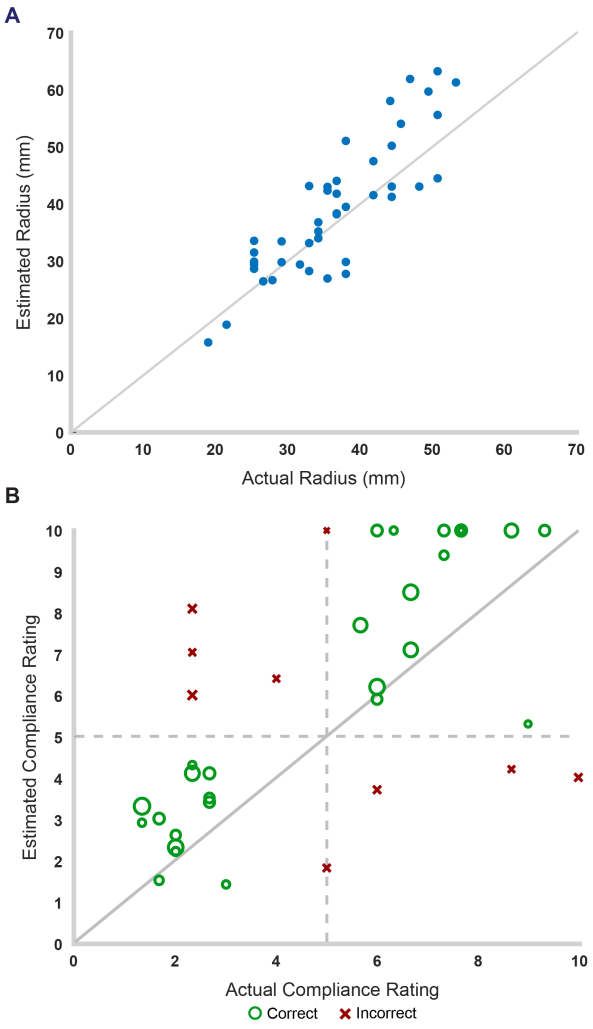

Fig. 5. Comparison of the estimated grasped object properties with ground truth based on strain and pressure sensor readings. The estimated radius showed a tight linear correlation with the actual radius (A), while the estimated compliance rating could do a binary classification of hard vs. soft objects (B). In both graphs, the dark gray line is $y = x$, where estimated equals actual measurement. In (B), the size of the marker corresponds to the size of the grasped object while the dashed lines represent the "hard / soft" boundary.

compliance meant that more soft items were classified as 10, making the system not have as much granular resolution as desired.

We also found a slight correlation in compliance accuracy to the size of object. As expected, our system was able to more accurately tell an object's compliance when the object was larger as the difference between a stiff and soft object would be more pronounced. We can see this slight effect in Fig. 5B, where the smaller sized markers tend to be further away from the ground truth line, especially for more compliant objects.

Although the estimated compliance ratings did not match as closely to the actual ratings as the radial measurements did, the binary classification was still sufficient to distinguish between similarly sized objects. For example, the pool noodle (radius 29 mm, compliance 8) and the rolling pin (radius 25 mm, compliance 3) optically appear very similar and were close enough in radius to potentially have their size differences be lost through noise. However, our estimated compliance for these objects were 9.4 and 1.4, respectively, a significant and sufficient difference to tell the objects apart.

VI. CONCLUSIONS AND FUTURE WORK

In this paper, we demonstrated a new soft gripper with proprioceptive sensing capabilities that is fully electrically actuated. By designing the gripper with scalability in mind, this gripper avoids the bulkiness of fluidic driven soft actuators and the stiffness of rigid-material grippers with compliant drive-trains. This gripper is able to grasp a wide range of objects with a simple open-loop control scheme and sort these objects based on object radius and compliance. Out of 56 total objects, 77% could be grasped and have size estimated to within 30% of actual size, while 78% of non-metal objects could be classified as hard / soft with 78% accuracy.

Future work on this system will focus on better understanding and improved design of the pressure sensors to address more complex applications. Although the pressure sensors show potential and sufficient sensitivity, more characterization is needed to fully understand what affects their measurements. For example, the pressure sensors are sensitive enough to detect in-hand object shifting between the two fingers, but we do not yet know how to characterize the motion. Creating an addressable array of pressure sensors would be a good first step to answering these questions.

We would also like to integrate the tactile information of this gripper with existing vision-based manipulation systems. Supplementing a visual inspection of grasped object with direct tactile information could lead to more dexterous manipulation and less time spent training to recognize how to grasp new objects.

ACKNOWLEDGMENTS

This work was completed with support from Amazon, JD, the Toyota Research Institute (TRI), and the National Science Foundation, grant #1830901. LC was supported under the National Science Foundation Graduate Research Fellowship grant #1122374, the Paul & Daisy Soros Fellowship for New Americans, and the Fannie and John Hertz Foundation. MCY was supported by the Laura Winkelman Davidson Fellowship from Purdue University and a NASA STTR Phase II contract (80NSSC17C0030). This article solely reflects the opinions and conclusions of its authors and not that of its sponsors.

The authors would like to thank Jonathan Tagoe for improving the process for laser cutting the HSAs, and Jonathan Zong for helping with data collection.

REFERENCES

[1] D. Rus and M. T. Tolley, "Design, fabrication and control of soft robots," *Nature*, vol. 521, no. 7553, pp. 467–475, May 2015.

[2] F. Iida and C. Laschi, "Soft Robotics: Challenges and Perspectives," *Procedia Computer Science*, vol. 7, pp. 99–102, Jan. 2011.

[3] J. Hughes, U. Culha, F. Giardina, F. Guenther, A. Rosendo, and F. Iida, "Soft Manipulators and Grippers: A Review," *Frontiers in Robotics and AI*, vol. 3, Nov. 2016.

[4] J. Shintake, V. Cacucciolo, D. Floreano, and H. Shea, "Soft Robotic Grippers," *Advanced Materials*, vol. 30, no. 29, p. 1707035, 2018.

[5] L. U. Odhner, L. P. Jentoft, M. R. Claffee, N. Corson, Y. Tenzer, R. R. Ma, M. Buehler, R. Kohout, R. D. Howe, and A. M. Dollar, "A compliant, underactuated hand for robust manipulation," *The International Journal of Robotics Research*, vol. 33, no. 5, pp. 736–752, Apr. 2014.

[6] B. S. Homberg, R. K. Katzschmann, M. R. Dogar, and D. Rus, "Haptic identification of objects using a modular soft robotic gripper," in *Intelligent Robots and Systems (IROS), 2015 IEEE/RSJ International Conference On*. IEEE, 2015, pp. 1698–1705.

[7] H. Zhao, K. O'Brien, S. Li, and R. F. Shepherd, "Optoelectronically innervated soft prosthetic hand via stretchable optical waveguides," *Science Robotics*, vol. 1, no. 1, p. eaai7529, Dec. 2016. [Online]. Available: http://robotics.sciencemag.org/content/1/1/eaai7529

[8] R. L. Truby, M. Wehner, A. K. Grosskopf, D. M. Vogt, S. G. M. Uzel, R. J. Wood, and J. A. Lewis, "Soft Somatosensitive Actuators via Embedded 3D Printing," *Advanced Materials*, vol. 30, no. 15, p. 1706383.

[9] R. A. Bilodeau, E. L. White, and R. K. Kramer, "Monolithic fabrication of sensors and actuators in a soft robotic gripper," in *Intelligent Robots and Systems (IROS), 2015 IEEE/RSJ International Conference on*. IEEE, 2015, pp. 2324–2329.

[10] P. Polygerinos, N. Correll, S. A. Morin, B. Mosadegh, C. D. Onal, K. Petersen, M. Cianchetti, M. T. Tolley, and R. F. Shepherd, "Soft Robotics: Review of Fluid-Driven Intrinsically Soft Devices; Manufacturing, Sensing, Control, and Applications in Human-Robot Interaction," *Advanced Engineering Materials*, vol. 19, no. 12, Dec. 2017.

[11] C. Laschi, B. Mazzolai, and M. Cianchetti, "Soft robotics: Technologies and systems pushing the boundaries of robot abilities," *Science Robotics*, vol. 1, no. 1, p. eaah3690, Dec. 2016.

[12] S. I. Rich, R. J. Wood, and C. Majidi, "Untethered soft robotics," *Nature Electronics*, vol. 1, no. 2, pp. 102–112, Feb. 2018.

[13] L. Chin, J. Lipton, R. MacCurdy, J. Romanishin, C. Sharma, and D. Rus, "Compliant electric actuators based on handed shearing auxetics," in *2018 IEEE International Conference on Soft Robotics (RoboSoft)*, Apr. 2018, pp. 100–107.

[14] M. C. S. Yuen, T. R. Lear, H. Tonoyan, M. Telleria, and R. Kramer-Bottiglio, "Toward Closed-Loop Control of Pneumatic Grippers During Pack-and-Deploy Operations," *IEEE Robotics and Automation Letters*, vol. 3, no. 3, pp. 1402–1409, July 2018.

[15] S. Montambault and C. M. Gosselin, "Analysis of Underactuated Mechanical Grippers," *Journal of Mechanical Design*, vol. 123, no. 3, p. 367, 2001.

[16] A. M. Dollar and R. D. Howe, "Joint Coupling Design of Underactuated Grippers," in *Volume 2: 30th Annual Mechanisms and Robotics Conference, Parts A and B*, vol. 2006. Philadelphia, Pennsylvania, USA: ASME, 2006, pp. 903–911.

[17] M. Grebenstein, M. Chalon, W. Friedl, S. Haddadin, T. Wimböck, G. Hirzinger, and R. Siegwart, "The Hand of the DLR Hand Arm System: Designed for Interaction," *Int. J. Rob. Res.*, vol. 31, no. 13, pp. 1531–1555, Nov. 2012.

[18] J. M. Romano, K. Hsiao, G. Niemeyer, S. Chitta, and K. J. Kuchenbecker, "Human-Inspired Robotic Grasp Control With Tactile Sensing," *IEEE Transactions on Robotics*, vol. 27, no. 6, pp. 1067–1079, Dec. 2011.

[19] M. V. Liarokapis, B. Calli, A. J. Spiers, and A. M. Dollar, "Unplanned, model-free, single grasp object classification with underactuated hands and force sensors," in *2015 IEEE/RSJ International Conference on Intelligent Robots and Systems (IROS)*, Sept. 2015, pp. 5073–5080.

[20] M. Issa, D. Petkovic, N. D. Pavlovic, and L. Zentner, "Sensor elements made of conductive silicone rubber for passively compliant gripper," *The International Journal of Advanced Manufacturing Technology*, vol. 69, no. 5, pp. 1527–1536, Nov. 2013.

[21] L. Wang, J. DelPreto, S. Bhattacharyya, J. Weisz, and P. K. Allen, "A highly-underactuated robotic hand with force and joint angle sensors," in *2011 IEEE/RSJ International Conference on Intelligent Robots and Systems*, Sept. 2011, pp. 1380–1385.

[22] N. Farrow, Y. Li, and N. Correll, "Morphological and Embedded Computation in a Self-contained Soft Robotic Hand," *arXiv:1605.00354 [cs]*, May 2016, arXiv: 1605.00354.

[23] V. Wall, G. Zöller, and O. Brock, "A method for sensorizing soft actuators and its application to the RBO hand 2," in *2017 IEEE International Conference on Robotics and Automation (ICRA)*, May 2017, pp. 4965–4970.

[24] B. Shih, D. Drotman, C. Christianson, Z. Huo, R. White, H. I. Christensen, and M. T. Tolley, "Custom soft robotic gripper sensor skins for haptic object visualization," in *2017 IEEE/RSJ International Conference on Intelligent Robots and Systems (IROS)*, Sept. 2017, pp. 494–501.

[25] J. Morrow, H. S. Shin, C. Phillips-Grafflin, S. H. Jang, J. Torrey, R. Larkins, S. Dang, Y. L. Park, and D. Berenson, "Improving Soft Pneumatic Actuator fingers through integration of soft sensors, position and force control, and rigid fingernails," in *2016 IEEE International Conference on Robotics and Automation (ICRA)*, May 2016, pp. 5024–5031.

[26] J. I. Lipton, R. MacCurdy, Z. Manchester, L. Chin, D. Cellucci, and D. Rus, "Handedness in shearing auxetics creates rigid and compliant structures," *Science*, vol. 360, no. 6389, pp. 632–635, May 2018.

[27] W. Felt and C. David Remy, "A Closed-Form Kinematic Model for Fiber-Reinforced Elastomeric Enclosures," *Journal of Mechanisms and Robotics*, vol. 10, no. 1, pp. 014 501–014 501–6, Nov. 2017.

[28] F. Ilievski, A. D. Mazzeo, R. F. Shepherd, X. Chen, and G. M. Whitesides, "Soft Robotics for Chemists," *Angewandte Chemie*, vol. 123, no. 8, pp. 1930–1935, Feb. 2011.

[29] E. L. White, M. C. Yuen, J. C. Case, and R. K. Kramer, "Low-Cost, Facile, and Scalable Manufacturing of Capacitive Sensors for Soft Systems," *Advanced Materials Technologies*, vol. 2, no. 9, p. 1700072, Sept. 2017.

[30] J. C. Case, J. Booth, D. S. Shah, M. C. Yuen, and R. Kramer-Bottiglio, "State and stiffness estimation using robotic fabrics," in *2018 IEEE International Conference on Soft Robotics (RoboSoft)*, Apr. 2018, pp. 522–527.

[31] B. Calli, A. Singh, A. Walsman, S. Srinivasa, P. Abbeel, and A. M. Dollar, "The ycb object and model set: Towards common benchmarks for manipulation research," in *Advanced Robotics (ICAR), 2015 International Conference on*. IEEE, 2015, pp. 510–517.